PHYSICAL REVIEW A VOLUME 2, NUMBER 4 OCTOBER 1970

Angular Distribution of Protons and Deuterons Produced by Dissociative Ionization of H_2 and D_2 near Threshold*

R. J. Van Brunt† and L. J. Kieffer‡
Joint Institute for Laboratory Astrophysics, University of Colorado, Boulder, Colorado 80302
(Received 6 February 1970)

From observations of the kinetic-energy distribution of protons and deuterons at corresponding forward and backward angles with respect to the electron-beam direction, the forward momentum imparted to the dissociating H_2 (D_2) molecule by the incident electron has been determined for electron energies up to 300 eV. The momentum transfer along the beam was found to remain nearly constant at all energies above threshold, although above 100 eV the values obtained for D_2 were systematically higher than the values for H_2. When corrected to the center-of-mass system, the angular distribution of H^+ (D^+) near threshold was found to contain a large isotropic component and an anisotropic component which deviates, in a manner suggested by Zare, from the $\cos^2\Theta$ dependence predicted from a simple dipole Born approximation.

I. INTRODUCTION

When a molecular gas is bombarded with electrons of sufficient energy to cause dissociation, the angular distribution of the fragments will, in general, be anisotropic with respect to the direction of incidence. This fact was first realized by Dunn,[1] who demonstrated that the angular distribution of the products of dissociation produced by electron impact depends critically on the symmetries of the initial and final molecular electronic states involved in the process. A subsequent measurement by Dunn and Kieffer,[2] as well as a much earlier observation by Sasaki and Nakao,[3] demonstrated that these arguments apply to dissociative ionization of H_2. Dunn and Kieffer attempted to explain the observed electron energy dependence of the angular distribution of fast protons from H_2 for electron energies above 50 eV in terms of a simple dipole Born approximation. More recently Zare,[4] following closely an earlier Born-approximation treatment of Kerner,[5] calculated the angular distribution of H^+ from dissociation of H_2^+ by electron impact, a process which, except for the absence of an additional ejected electron, should be quite similar to that of dissociative ionization. He argued from a consideration of the momentum transfer involved, that the angular distribution of H^+ from H_2 near threshold should deviate appreciably from the $\cos^2\Theta$ dependence predicted by the dipole approximation.

The effect of the momentum transferred to the heavy particles by the incident electron was not included in the interpretation of Dunn and Kieffer's[2] results. Recent experimental evidence,[6,7] however, suggests that heavy-particle recoil can be an important factor in determining the mechanics of atomic and molecular excitation and ionization processes produced by electron impact, even at energies much above threshold. A careful consideration of this effect is therefore essential, especially when explaining laboratory observations of processes involving relatively light atoms or molecules. In the present paper, the measurements of Dunn and Kieffer have been repeated and extended to threshold to learn more about the effect of molecular recoil on the angular energy distribution of H^+ (D^+), as well as to determine the validity of the dipole approximation as it applies to this process.

II. APPARATUS

The apparatus used in this experiment is similar to the one used by Dunn and Kieffer.[2] However, several significant improvements were made, the most important being a large increase in sensitivity through the use of counting techniques. The collision chamber, electron gun, ion optics, and vacuum system were completely redesigned for this experiment. Figure 1 shows a detailed scale drawing of the collision chamber and electron gun which were mounted inside a stainless-steel vacuum system.

A well-collimated low-energy electron beam produced ions in a field-free region which then drifted under their initial velocity through a pair of apertures (A1 and A2) into a 60° sector magnet. The magnet was tuned to select ions of a particular momentum which were then accelerated and focused into an electron multiplier. The output pulses of the multiplier were amplified and counted with a scaler. The electron gun was rotatable with

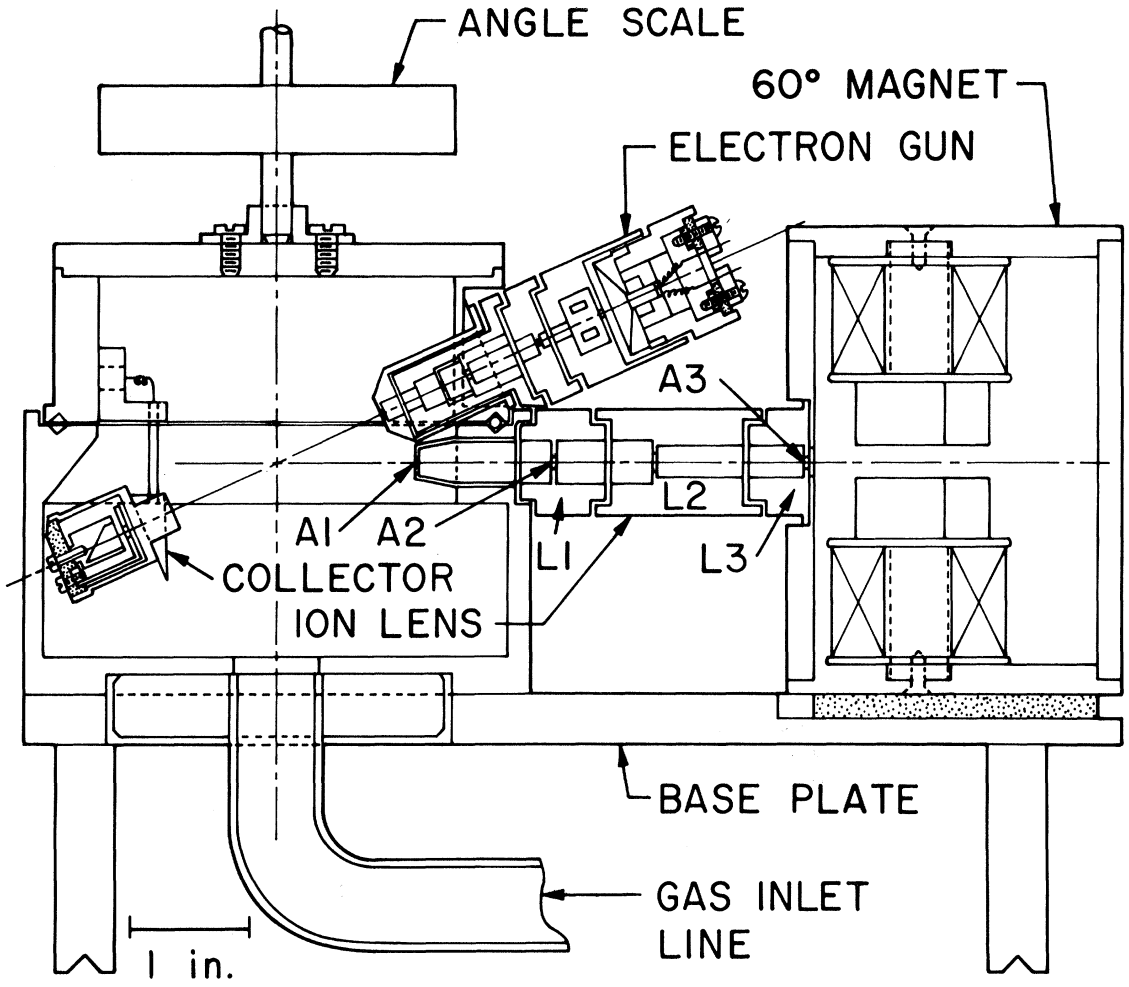

FIG. 1. Collision chamber, electron gun, ion lens, and spectrometer.

respect to the ion-detection system in such a way that measurements of ion intensity could be performed in the laboratory angular ranges $157^\circ \geq \Theta \geq 23^\circ$ and $337^\circ \geq \Theta \geq 203^\circ$. By varying the field in the 60° sector magnet, a measure of the momentum distribution of the ions could be obtained.

The collision chamber was machined out of 304 stainless steel and consisted of two sections. The bottom section was bolted to a base plate which supported the spectrometer and ion-lens systems, and the top section, to which the electron gun was attached, rotated with respect to the bottom section on three small sapphire ball bearings evenly spaced in a circular V groove and lubricated with pure powdered tungsten disulfide. Rotation was performed by means of a vacuum mechanical feedthrough connected to the scattering chamber by a flexible steel shaft. The top section could rotate 360° with respect to the bottom section. The electron gun's angle of orientation was measured by observing a scale rigidly attached to the rotating section with a telescope located outside the vacuum chamber.

The electron-gun axis was oriented at an angle of 23° with respect to the plane perpendicular to the rotation axis. Precision mechanical measurements indicated that the axis of the chamber, gun, and ion-lens system always intersected to within a sphere of diameter 0.001 in. The laboratory angle Θ between the electron-beam axis and ion-lens axis is related to the angle of rotation of the collision chamber γ by a simple transformation

$$\cos\Theta = \cos 23^\circ \cos\gamma . \tag{1}$$

The electron gun was similar in design to one discussed by Kuyatt and Simpson[8] which employed a multistaging technique, whereby electrons were drawn from a cathode by a high potential and then decelerated to the final energy. It was specifically

designed to operate at low energies in the range 5–300 eV and to produce a well-collimated beam with total divergence angle less than 2.0° at all energies. The maximum beam current obtained depended on energy and varied from about 0.15 μA at 6.0 V to 20 μA at 150 V. Beam currents in excess of 20 μA were never used. At each electron energy the voltage ratio on each lens of the gun was adjusted to give proper focus which could be determined by observing the current arriving at the collecting cup and an aperture ring placed in front of the cup (see Fig. 1). The electron-collector aperture was just large enough to pass the space-charge-limited current for a beam 6.0 cm in length, corresponding to the distance between this aperture and the exit aperture of the gun. The voltage ratio on the final electron-gun lens was adjusted to minimize current to the ring and maximize current to the cup. By applying a retarding potential to the collector aperture ring, a rough measure of the energy spread of the electron beam was obtained and found to be approximately 0.5 eV.

The interaction region was totally shielded from electric fields produced by the electron-gun and ion-lens elements. Morever, the gun, magnet, and ion-lens system were "self-shielding" so that fields generated by one could not influence the operation of the other. The earth's magnetic field as well as small fields produced by the 60° sector magnet and ion pump were shielded out with a double layer of Co-Netic AA foil. The 60° sector spectrometer was designed so that its field dropped off extremely rapidly at short distances beyond its entrance and exit apertures. With no current passing through the magnet coils, the maximum magnetic field measured in the center of the collision chamber was 0.035 G. As the field in the spectrometer was increased from 0 to 1 kG, the field inside the scattering chamber was observed to change by about 0.02 G.

All of the stainless-steel parts close to the electron beam, such as the electron-collector shield, were thoroughly demagnetized before assembly. To avoid possible effects due to surface charge, the insulators used to support the electron collector and the first ion-lens system were well shielded from the beam and interaction region. The inside surfaces of the scattering chamber, ion lens, and magnet were coated with aquadag (colloidal carbon) to reduce contact potentials and surface reflection of electrons. The surfaces of the electron collector were coated with platinum black.

The angular resolution was determined by the size and spacing of the apertures A1 and A2 and estimated to be ±1.2°. Except for a few minor mechanical modifications, the 60° sector magnet was identical to the one used by Dunn and Kieffer.[2] From a consideration of the effective radius of curvature of the magnet and the size of the exit aperture the calculated energy resolution of the spectrometer for a parallel ion beam was $\Delta E/E = 0.13$. An examination of ion peak widths obtained from mass scans of accelerated thermal-energy ions gave a value of 0.10 for $\Delta E/E$.

The vacuum chamber in which the instrument was placed was evacuated with a 50-liter/sec ion pump and a titanium sublimator with an estimated effective pumping speed for H_2 and D_2 of about 640 liters/sec. The gas to be studied was introduced through a stainless-steel tube connected directly to the bottom of the collision chamber as shown in Fig. 1. Under normal operating conditions, the gas pressure inside the collision chamber was between two and three orders of magnitude greater than the pressure outside. This pressure was monitored with an ion gauge located in the gas inlet line and controlled by a variable leak connected to a high-purity gas sample contained in a 1-liter glass flask at 1-atm pressure. A bypass valve permitted evacuation of the gas line at times when the leak was closed, and prior to introducing the sample, the line was uniformly baked at a temperature of about 200 °C.

The base pressure of the system was 3.5×10^{-8} Torr. With gas in the collision chamber at 5×10^{-5} Torr the sublimator filament was turned on at least once every 15 min for a period of about 0.5 min. This was sufficient to maintain the pressure outside the collision chamber at a value below 10^{-7} Torr. The sublimator filament was never on when data were taken, although its operation appeared to have no effect on the positive-ion count rate.

III. EXPERIMENTAL RESULTS AND DATA ANALYSIS

A. General

Three types of measurements could be made with this instrument: (a) the momentum distribution of ions for a fixed electron energy and angle, (b) the angular distribution of ions for a fixed electron energy and ion momentum, and (c) the appearance potential of ions from a measurement of ion count versus electron energy for a fixed ion momentum and angle.

B. Kinetic-Energy Distributions of H^+ and D^+ from H_2 and D_2

The kinetic energy E of an ion of mass M was measured using the first-order focusing condition of a 60° sector magnet given by $E = B^2/M\alpha^2$, where B is the magnetic field strength and α is a geometrical factor. The method of experimentally determining α as well as contact potential corrections is identical to that used previously.[2,9] The observed

deviation in α gave an uncertainty of $\pm 2.0\%$ in the ion-energy scale. The contact potential correction was measured on each day that data were taken and was found to be around $+0.15$ V for H_2 in the system whereas a systematically lower correction of about -0.04 V was obtained with D_2 in the system. Although the accuracy of the energy scale in this experiment depended on the magnet calibration, an independent check on the energy scale was made by observing the position of mass peaks which result from accelerating ions with initially thermal energy (e.g., H_2^+ and D_2^+) into the spectrometer by applying an accurately measured potential to V_{L3}. A comparison of the energy scale determined in this way always agreed to within 0.2 V with that predicted from the magnet calibration. Measurements of energy distributions made at the same angle and electron energy on different days also agreed to within 0.2 eV.

It should be emphasized that when ion kinetic energies were measured, no potentials were applied to the ion-lens elements to draw ions out of the interaction region or focus them into the spectrometer. The ions which entered the spectrometer and subsequently the multiplier drifted through apertures A1 and A3 under their own velocity. Focusing voltages were applied to the ion-lens elements only when measurements were made of the mass spectra of accelerated thermal-energy ions.

The electron energy scale was determined from retarding measurements of the beam as well as from appearance potential measurements of the ions H_2^+ and D_2^+ with known ionization energies. The estimated error in determining the electron energy scale was ± 0.2 eV, which mainly corresponds to the error in measuring ionization potentials due to the energy spread in the electron beam.

Each data run for kinetic-energy distributions consisted of an average of two or more successive magnet scans made by measuring the ion count at fixed intervals of the magnet current. The magnet was recycled before each scan. The integration time at each magnet current setting was determined by the electron-beam current measured at the collector. The current arriving at the collecting cup plus aperture ring was measured with a 610 B Keithley electrometer used to drive a voltage-to-frequency converter which produced an output frequency proportional to the electron-beam current. This frequency was counted with a scaler, the output of which was used to control a gating circuit that determined the period during which ions were counted. In this way the data were automatically corrected for variations in electron-beam current. The dependence of ion count on beam current was found to be linear over the range of currents used. This indicated that there was essentially no trapping of ions in the beam, which is expected, since the estimated potential well depth of a 35-V electron beam at a current of 4 μA, corresponding to the conditions normally achieved, is about 0.17 V, an order of magnitude lower than the lowest ion energy observed.

The measurements on H_2 and D_2 were typically performed at collision-chamber pressures slightly below 5×10^{-5} Torr, as measured with an ion gauge in the gas inlet line. Measurements of the H^+ and D^+ count rate at different angles and energies as a function of chamber pressure yielded a linear dependence below 2×10^{-4} Torr with zero intercept. During each data run the pressure was monitored on a strip chart recorder. Variations in pressure greater than $\pm 1\%$ were never permitted; moreover, the effect of small pressure drift was essentially averaged out by the method of taking data.

The data shown in Figs. 2–4 and 6 were arbitrarily normalized to the peak ion count. To obtain the curves of Figs. 3 and 4, a line was drawn through the data points which had been corrected for spectrometer resolution in a manner previously described,[10] i.e., the observed ion count at each mag-

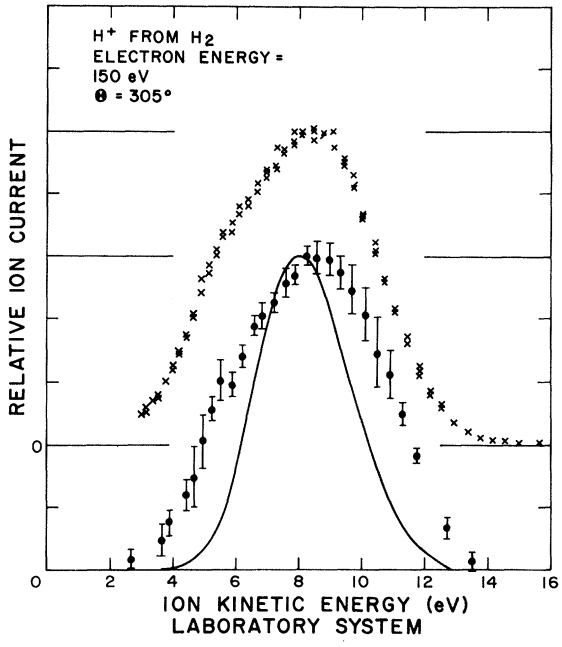

FIG. 2. Kinetic-energy distribution of H^+ from H_2 for $E_e = 150$ eV and $\Theta = 305°$. The dots with error bars correspond to the data of Kieffer and Dunn (Ref. 9) and the crosses are the present result. The solid line represents a theoretical Franck-Condon prediction (Ref. 9) which has been corrected for spectrometer resolution and molecular thermal motion and is based on the assumption that the observed H^+ ions come only from the $^2\Sigma_u^+$ repulsive state of H_2^+.

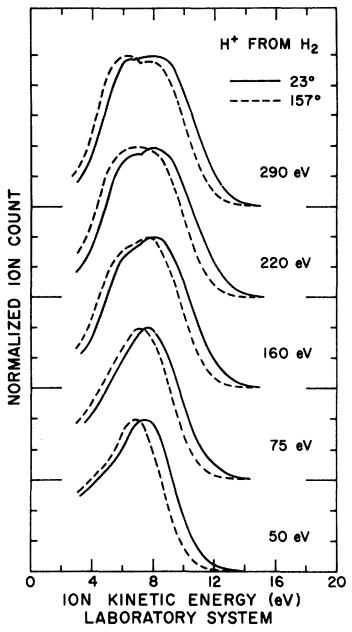

FIG. 3. Observed kinetic-energy distributions of H^+ from H_2 at different electron energies for $\Theta = 23°$ (solid lines) and $\Theta = 157°$ (dashed lines). The corresponding electron energies are indicated at the right of each pair of lines.

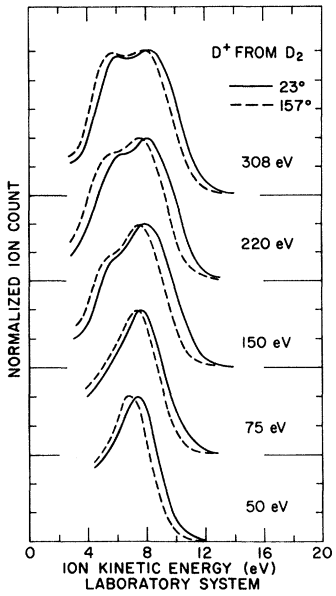

FIG. 4. Observed kinetic-energy distributions of D^+ from D_2 at different electron energies for $\Theta = 23°$ (solid lines) and $\Theta = 157°$ (dashed lines). The corresponding electron energies are indicated at the right of each pair of lines.

net setting was divided by the calculated energy which the ions had when they passed through the spectrometer. In order to compare with the results of Kieffer and Dunn, [9] the data shown in Figs. 2, 5, and 6 were not corrected for the effect of spectrometer resolution. The energy-distribution curves shown in Figs. 2–4 represent data from single runs in which the degree of scatter is indicated by the crosses in Fig. 2. Repeated measurements demonstrated that the shapes of the distribution curves were quite reproducible.

Appearance potential measurements made at ion energies above 3.0 eV did not reveal any structure which might be attributed to the presence of background ions. Mass spectra of accelerated thermal-energy ions identified the contaminants in the vacuum system to be mainly H_2O, CO, N_2, CO_2, and Ar, listed in order of observed intensity. A comparison of mass peak heights indicated that the relative concentrations of these ions were less than 1.0% of H_2 or D_2. The base pressure in the gas line was $\sim 4\times10^{-8}$ Torr, and the impurity content of the gas samples used was given by the manufacturer as 25 ppm. Magnet scans of unaccelerated ions performed without H_2 or D_2 in the system showed that energetic ions produced from the background gas were of high momentum and most intense at magnet currents far above the range where H^+ and D^+ were observed.

The energy-distribution measurements of Kieffer and Dunn[9] were repeated in the present experiment for the same angle and electron energy in order to obtain a check on the energy scale and to verify the shape of the distribution which they observed. The results for H^+ are shown in Fig. 2, in which the

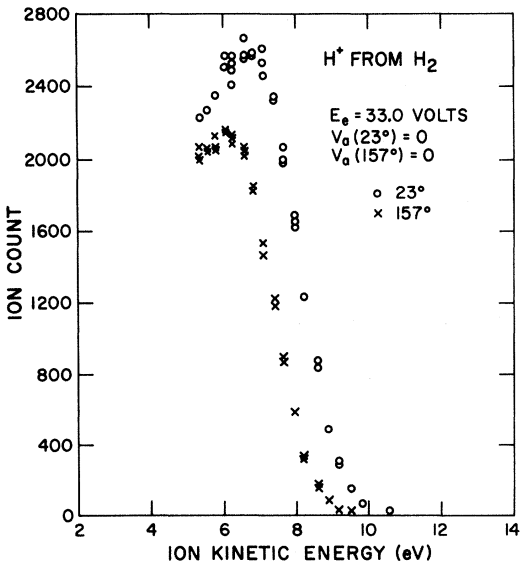

FIG. 5. Kinetic-energy distributions of H^+ from H_2 near threshold for $E_e = 33.0$ eV and $V_a(23°) = V_a(157°) = 0$.

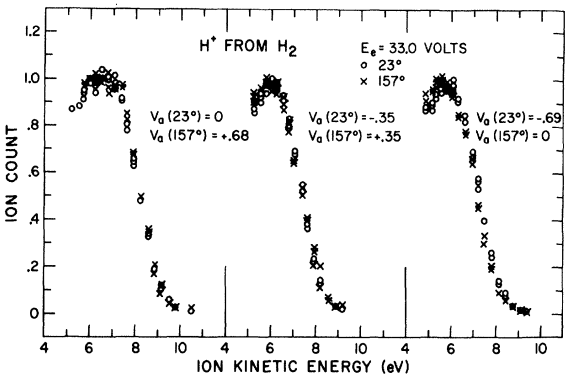

FIG. 6. Kinetic-energy distributions of H^+ near threshold for $E_e = 33.0$ eV. The ions were accelerated or retarded (+ or −) by the potential V_a applied to the spectrometer. Each set of data was taken on a different day and the three sets were then normalized by setting their peak values equal to 1.0. V_a is in volts.

dots with error bars correspond to their measurement and the crosses correspond to the present data. The solid line in this figure is a theoretical energy-distribution curve predicted by Kieffer and Dunn[9] using Franck-Condon overlaps and assuming that the ions are produced by a transition from the ground Σ_g^+ state of H_2 to the repulsive Σ_u^+ state of H_2^+. For purposes of comparison, the theoretical curve was corrected for the effects of the molecular thermal-velocity distribution and the finite-energy resolution of the spectrometer. Neither set of experimental data has been corrected for the spectrometer resolution. The results obtained agree with those of Kieffer and Dunn, although there is a slight difference of about 0.25 eV in the energy scales, which is within the stated error for both experiments.

Figures 3 and 4 show a comparison of energy-distribution curves for H^+ and D^+ taken on the same day at the corresponding forward and backward laboratory angles $\Theta = 23°$ and $\Theta = 157°$ for different incident electron energies. The significant features of these data are the variations in structure of the distribution curves with electron energy and the forward and backward shift in energy which, as will be discussed later, is due to molecular recoil.

The data shown in Figs. 5 and 6 were taken at the same corresponding angles $\Theta = 23°$ and $\Theta = 157°$ at an electron energy near the threshold for formation of ions with a center-of-mass kinetic energy of about 8.0 eV.

C. Measurement of Molecular Recoil

Upon colliding with an electron, a molecule will acquire an additional velocity due to momentum transfer, and its kinetic energy will change by an amount δE which satisfies the condition $\delta E \leq 4\,(m_e/M)E_e$, where m_e is the electronic mass, M is the molecular mass, and E_e is the incident electron energy. The equality corresponds to the 180° elastic scattering. If the electron loses all of its energy in the collision such as occurs in an ionization or excitation process at threshold, then $\delta E = (m_e/M)E_e$. For an incident energy of 35.0 eV, the maximum kinetic-energy change for the molecules H_2 and D_2 is on the order of the mean thermal energy at room temperature (300 °K); hence the effect of molecular recoil would ordinarily be difficult to observe. However, if the molecule dissociates after the collision, the momentum transferred to the molecule may appear as a relatively large shift in the kinetic energy of the dissociation fragments. For a process such as dissociative ionization at threshold, one can argue from conservation of energy that the electron is stopped and all of its momentum is imparted to the heavy particles. From simple classical kinematical considerations, it can be shown for the process of dissociative ionization at threshold that the difference between the kinetic energy of dissociation products formed with the same center-of-mass energy E_0 but observed at the corresponding laboratory angles Θ and $\pi - \Theta$ is given to a good approximation by

$$\Delta E\,(\Theta) = 4\,(M_A/M_{AB})\{(m_e/M_A)(1 - M_A/M_{AB}) \times [E_e^2 - E_e\,(D + I)]\}^{1/2}\cos\Theta, \qquad (2)$$

where M_A is the mass of the fragment, M_{AB} is the mass of the molecule, D is the dissociation energy of the molecular ion, and I is the ionization potential of the molecule. In deriving Eq. (2), the condition for energy and momentum balance has been used, namely,

$$E_0 = (1 - M_A/M_{AB})\,[E_e - (D + I)] \quad . \qquad (3)$$

Equation (2) is valid if $E_0 \gg \delta E$, a condition well satisfied for dissociative ionization from the repulsive $^2\Sigma_u^+$ state of H_2^+ and D_2^+, since $\delta E \sim 0.04$ eV, whereas $E_0 \sim 8.0$ eV. At threshold for H^+ formation from H_2 by 33-eV electrons, Eq. (2) gives $\Delta E\,(0°) = 0.73$ eV, where the values $I = 15.42$ eV and $D = 2.65$ eV have been used.

The energy-distribution data shown in Fig. 5 demonstrate that there is indeed an observable shift in the kinetic energy of this magnitude near threshold. An accurate measure of the energy shift $\Delta E(23°)$ cannot, however, be obtained from these data because of the intensity difference in the ion count at the two angles resulting from the fact that no correction has been applied for the effect of spectrometer resolution. Note that the ratio of the peak heights is roughly equal to the ratio of corresponding peak energies. At threshold the energy shift $\Delta E\,(\Theta)$ was

measured in two ways: (a) by applying a small retarding or accelerating potential V_a to the spectrometer (lens element L3 of Fig. 1) relative to the collision chamber necessary to bring the energy-distribution curves into agreement at the corresponding angles Θ and $\pi - \Theta$; and (b) by determining the shift in the energy-distribution curves obtained without applying potentials to the spectrometer, but correcting for the effect of spectrometer resolution. Both methods gave the same value for the same conditions of electron energy and angle. Figure 6 illustrates the degree to which energy-distribution curves near threshold could be brought into agreement by applying potentials V_a to the spectrometer, and shows that these voltages left the shape of the distribution curves essentially unchanged. This is expected since the energy shifts are about an order of magnitude smaller than the mean ion kinetic energy, which implies that focusing effects in the lens system were quite small. The accelerating and retarding potentials used to obtain the data in Fig. 6 include the largest ever applied, and therefore, this figure represents the "worst" conditions. The three sets of data shown were taken on different days. For the first set (left-hand side of Fig. 6), agreement was obtained by applying an accelerating potential with $\Theta = 157°$. For the third set, a retarding potential was applied with $\Theta = 23°$, and for the second, both retarding and accelerating voltages were used.

The forward-backward energy shift given by Eq. (2) is obtained from the potentials V_a using the formula

$$\Delta E(\Theta) = V_a(\Theta) - V_a(\pi - \Theta) .$$

Thus variations in the values for V_a shown in Fig. 6 give a measure of the uncertainty in determining ΔE, which in this case is about ± 0.02 V. The experimental values for ΔE, determined by the above instrumental techniques, agreed well with the theoretical values predicted from Eq. (2), thus verifying that the observed energy shift is indeed that due to the effect of momentum transferred to the molecule by the incident electron. The measurements on D^+ produced a value for ΔE which was scaled down from the H^+ value by a factor of $1/\sqrt{2}$ as predicted. Moreover, the measurements of $\Delta E(\Theta)$ at threshold for different Θ showed the proper $\cos\Theta$ dependence given by Eq. (2). This is demonstrated by the data in Fig. 7. A small error is introduced by this method of determining the energy shift due to neglect of correction terms which arise in transforming from the center of mass to the laboratory system.[11] The observed energy shifts are therefore slightly larger than predicted at threshold.

The momentum transferred to the dissociating molecule at threshold can be calculated from the

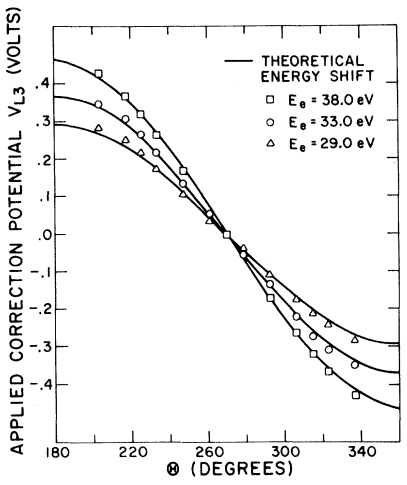

FIG. 7. Correction potentials applied to the spectrometer to remove the effects of momentum transfer. The solid line represents the theoretical energy shift. These data illustrate that the observed kinetic-energy shift of the H^+ ions near threshold has the correct angle dependence given by Eq. (2).

observed energy shift using the relationship

$$K = 5.8 \frac{\Delta E(\Theta)}{(E_0)^{1/2}} \frac{1}{\cos\Theta} , \qquad (4)$$

where K is the magnitude of the momentum transfer along the beam direction in units of reciprocal Bohr radii. Energy shifts measured at electron energies above threshold were also interpreted in terms of a mean momentum transferred to the molecule along the beam direction using Eq. (4). The results of such measurements are shown in Fig. 8 for both H_2 and D_2. Each point in this figure was obtained from a comparison of energy-distribution curves, such as shown in Figs. 3 and 4, taken on the same day at corresponding angles $\Theta = 23°$ and $\Theta = 157°$. The technique of retarding and accelerating ions was not used above threshold since the value of ΔE depended on E_0. However, attempts at taking data in this way were quite consistent with the results shown in Fig. 8. The arrows in this figure indicate the theoretical momentum transfer at threshold calculated using Eqs. (2) and (4) for formation of ions with center-of-mass kinetic energy E_0. The first point on the left of each set of data in Fig. 8 corresponds to the observed threshold value.

D. Measurement of Angular Distributions near Threshold

Figure 9 shows the angular distribution measurements of H^+ from H_2 near threshold which were instrumentally corrected to the center-of-mass system by applying accelerating and retarding voltages to the 60° spectrometer in the manner described

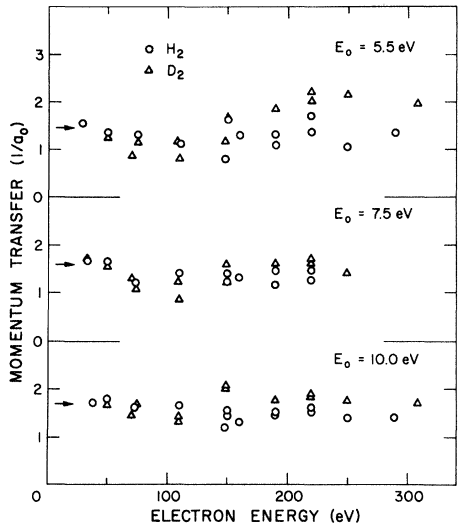

FIG. 8. Average momentum transferred to H_2 and D_2 along the electron-beam axis as a function of electron energy at different center-of-mass ion energies E_0 for the process of dissociative ionization. The first point corresponds to a measurement made at threshold, and the arrows indicate the theoretical threshold values.

above to compensate for the effect of momentum transferred to the molecule by the incident electron. This procedure for correcting angular distribution data to the center of mass is justified on the basis of the results presented above from the measurement of momentum transfer at threshold. The retarding or accelerating voltages applied to the spectrometer were adjusted to bring the ion count at Θ into agreement with that at $\pi - \Theta$. The actual voltages which were applied at threshold for three different electron energies are plotted in Fig. 7, as a function of angle, and compared with the kinetic-energy shift of H^+ ions predicted from Eq. (2). The applied correction potentials follow the theoretical energy-shift curves quite well, although, on the average, their magnitude is slightly larger than expected. The correction voltages required to give forward-backward symmetry for D^+ from D_2 were smaller by a factor of $1/\sqrt{2}$, consistent with the mass dependence of Eq. (2).

The data in Fig. 9 were obtained by multiplying the recorded ion count at each angle Θ by $\sin\Theta$ to correct for angular variations in the interaction volume, and then arbitrarily normalizing to 90°. The data runs were performed by first recording ion counts at odd values of the chamber angle γ for rotation in one direction, and then at even values of γ for rotation in the opposite direction. The period of a data run was typically 90 min. The points in Fig. 9 correspond to an average of five data runs taken on four different days on both sides of the collision chamber. The error bars represent the calculated standard deviations, and indicate the possible error in normalization.

Figure 10 shows angular distribution data which were taken without applying correction potentials to the spectrometer at electron energies of 50 and 75 eV for a laboratory ion energy of 8.6 eV. The results are compared with earlier measurements of Dunn and Kieffer,[2] performed in the same way under identical conditions. There appears to be reasonably good agreement with the same degree of forward-backward asymmetry apparent in both sets of data. This asymmetry is consistent with the energy-distribution results shown in Fig. 3, and therefore easily accounted for in terms of molecular recoil. It should be noted, however, that an examination of the peak of the ion energy-distribution data taken at corresponding forward and backward angles at different electron energies and corrected for spectrometer resolution, revealed a slight forward-backward asymmetry independent of that accounted for by the energy shift due to momentum transfer. The magnitude of this asymmetry, defined by

$$[I(23°) - I(157°)] / I(23°),$$

was always less than 0.06 and could be associated with the effective variation of center-of-mass solid angle with laboratory angle Θ.[11] This effect may also explain why the applied correction potentials used at threshold (see Fig. 7) slightly exceeded the theoretically predicted values, i.e., the potentials "corrected" for this effect in addition to that due to

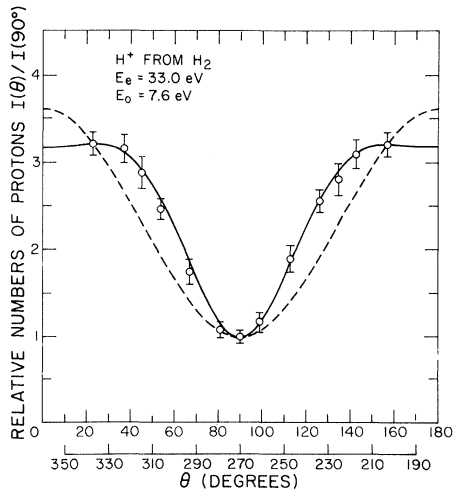

FIG. 9. Angular distribution of H^+ from H_2 at threshold for a center-of-mass ion energy of 7.6 eV and $E_e = 33.0$ eV. The solid line is a prediction using Eq. (8) derived by Zare (Ref. 4) for $K = 1.7$ $(1a_0)$ and $r_0 = 2a_0$. The dashed line represents the function $1.0 + 2.61\cos^2\theta$.

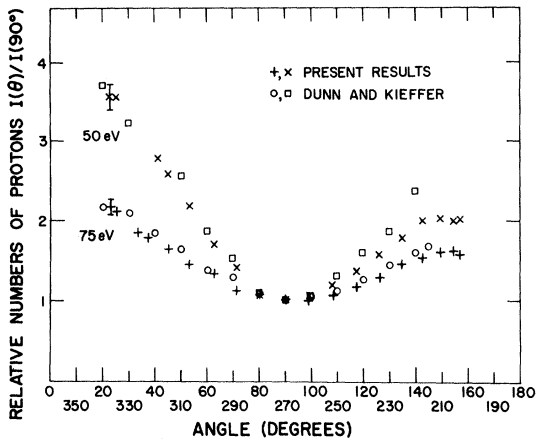

FIG. 10. Angular distribution of H^+ from H_2 for a laboratory ion energy of 8.6 eV at electron energies of 50 and 75 eV. The present results represented by the crosses and pluses are compared with the measurements of Dunn and Kieffer (Ref. 2). Neither set of data has been corrected for momentum transfer.

the energy shift. The results obtained serve to demonstrate that, in the laboratory system, the kinetic-energy shift of the dissociation products resulting from momentum given to the molecule by the electron is responsible for a forward-backward asymmetry in the angular distribution which depends on the ion energy (see Fig. 3), and becomes more pronounced as the electron energy approaches threshold.

IV. DISCUSSION OF RESULTS

A. Molecular Recoil

If the observed shift in the kinetic-energy distribution of H^+ and D^+ (see Figs. 3 and 4) is interpreted in terms of a mean molecular recoil along the beam direction, then the results in Fig. 8 indicate that it remains nearly constant for at least the first 300 eV above threshold. The momentum transfer is about the same for H_2 and D_2 from threshold to about 100 eV. Above this value, the points corresponding to D_2 appear to be systematically higher than those for H_2. At threshold for a given ion energy, the momenta transferred to the H_2 and D_2 molecules should be equal, as observed. Above threshold, there is no obvious reason why a difference could not occur. The fact that the forward component of the molecular recoil is essentially constant over a wide energy range is not physically unreasonable; however, no adequate theoretical explanation for this behavior has been found.

B. Angular Distribution in Center-of-Mass System

It can be shown from an expansion of the Born amplitude for a process involving excitation by electron impact from an initial molecular state U_0 to a final repulsive state U_n corresponding to an optically allowed transition, that the differential cross section is approximately given by [2,12,13]

$$\sigma_{\vec{K}} = A \left| \vec{K} \cdot \langle \vec{M} \rangle \right|^2 , \tag{5}$$

where A is a constant, $\langle \vec{M} \rangle$ is the dipole moment for the transition, and $\vec{K}$ is the momentum change vector for the electron. If $\vec{k}_0$ and $\vec{k}_n$ are, respectively, the initial and final momenta of the electron, then $\vec{K} = \vec{k}_0 - \vec{k}_n$. Equation (5) is a valid approximation only if $Kq \ll 1$, where q is the "range" of the product $U_n^* U_0$. If q is of the order a_0 (1 Bohr radius), as is usually the case, then we must have $K \ll 1/a_0$. Since Eq. (5) only applies to optically allowed transitions, the condition $\Delta\Lambda = 0, \pm 1$ must be satisfied, [14] where Λ is the component of the electronic angular momentum along the internuclear axis, which is a good quantum number for most molecules of interest. For an allowed $\Delta\Lambda = 0$ transition, the dipole moment lies along the internuclear axis, whereas for $\Delta\Lambda = \pm 1$ transitions it is perpendicular to the internuclear axis. Normally dissociation from an antibonding molecular state takes place in a time small compared to the period of rotation; thus the angular distribution of the dissociation products should reflect the initial orientation of the target molecules, and one can assume that the dissociation products fly apart along the internuclear axis, i.e., the case of axial recoil. [4,15] If the target molecules are randomly oriented in space and axial recoil assumed, then from Eq. (5) an allowed $\Delta\Lambda = 0$ transition gives rise to a $\cos^2\theta$ angular distribution of dissociation products with respect to the $\vec{K}$ axis and a $\Delta\Lambda = \pm 1$ transition gives a $\sin^2\theta$ distribution. At threshold for the excitation process, $\vec{K}$ lies along the direction of the incident electron, but above threshold, $\vec{K}$ has no fixed direction, although it may have a preferred direction. To obtain the differential cross section referred to, the beam direction Eq. (5) must be averaged over all possible values of $\vec{K}$. If the most probable angle between $\vec{K}$ and the incident electron direction $\vec{k}_0$ is θ', then it can be shown that a $\cos^2\theta$ distribution, when referred to the beam direction, takes the form [2,4,15]

$$I_{\vec{K}}(\theta, \phi) \sim (3\cos^2\theta' - 1)\cos^2\theta + \sin^2\theta' . \tag{6}$$

The case of dissociative ionization is complicated by the effect of the ejected electron, and the above arguments do not strictly apply. However, if the momentum transferred to the heavy particles can be neglected, then the ejected electron must travel predominantly in the direction of $-\vec{K}$ in order to conserve momentum. If this is true, then the symmetry axis is still defined by $\vec{K}$ and Eqs. (5) and (6)

apply to dissociative ionization.

For the transition from the ground $^1\Sigma_g^+$ state of H_2 to the repulsive $^2\Sigma_u^+$ state of H_2^+ the dipole approximation Eq. (5) predicts a $\cos^2\theta$ angular distribution of H^+ with respect to the incident electron direction at threshold. On the other hand, since the momentum transfer $\vec{K}$ for this process is rather large [$K \geq 1.4\,(1/a_0)$], there is really no apparent reason to believe, from a consideration of the arguments given above, that the dipole approximation should apply.

The threshold data of Fig. 9 can be described as a sum of an isotropic term plus an anisotropic term with a minimum at $\theta = 90°$. Attempts at fitting the anisotropic component with a $\cos^2\theta$ function were not successful, as is evident from the dashed line in this figure. These results, therefore, demonstrate that the dipole approximation does not adequately describe the angular dependence for dissociative ionization of H_2 near threshold. Measurements of the angular distribution of D^+ from D_2 gave the same result with the same degree of anisotropy. By analogy with his predictions for the process of dissociation of H_2^+ by electron impact, Zare[4] has suggested that the angular distribution of H^+ near threshold for dissociative ionization of H_2 could have the form

$$I_K(\theta, \phi) = F(K)\left| \sum_{l=1,3,5}^{\infty} (i)^l\,(2l+1)\,j_l(\tfrac{1}{2}Kr_0)\,P_l(\cos\theta) \right|^2, \tag{7}$$

where the j_l's are spherical Bessel functions and the $P_l(\cos\theta)$'s are Legendre polynomials. The first term in Eq. (7) gives the dipole contribution which should dominate for small values of Kr_0 where the approximation

$$j_l(\tfrac{1}{2}Kr_0) \simeq \left(\frac{1}{1\times 3\times\cdots\times(2l+1)}\right)(\tfrac{1}{2}Kr_0)^l \tag{8}$$

is valid. If the condition $Kr_0 \ll 1$ is not satisfied, as in the case of the process considered here, then higher-order terms in Eq. (7) become important in determining the form of the angular distribution. By considering the first five terms, Eq. (7) has been evaluated numerically using the values $r_0 = 2a_0$ and $K = 1.7\ (1/a_0)$ corresponding to the internuclear separation of the H_2 molecule and the experimentally observed momentum transfer for dissociative ionization (Fig. 8). For these values, the terms in Eq. (7) corresponding to $l \geq 7$ make a negligible contribution. The result of this calculation, shown by the solid curve in Fig. 9, fits the anisotropic component of the angular distribution well.[16] Excluding the isotropic component, this indicates that the theoretical description of the angular dependence for the process of dissociative ionization of H_2 must be quite similar to that for dissociation of H_2^+, which is expected if the effect of the additional outgoing electron for the ionization process is not very important close to threshold. Above threshold, the ejected electron could be important and may have some bearing on the observed isotropic component in the angular distribution. The molecular-recoil measurements indicate that a considerable portion of the incident electron's momentum is taken up by the heavy particles, even at energies far above threshold. This means that the ejected electron need not move predominantly along the direction of the momentum change vector, and, therefore, the symmetry axis about which the angular distribution is defined is not necessarily given by $\vec{K}$ as in Eq. (5). In this case, the symmetry properties of the two outgoing electrons can only be determined from a detailed solution of the scattering problem.

The isotropic component is difficult to explain since, theoretically, if the ions are produced only from a transition to the $^2\Sigma_u^+$ repulsive state, the differential cross section for H^+ formation should vanish at threshold for $\theta = 90°$. This is a consequence of the fact that, at threshold, both outgoing electrons have zero energy and angular momentum so that the wave functions describing each are spherically symmetric; and therefore the selection rules derived by Dunn[1] hold exactly. Several effects which could introduce an isotropic component in the data were investigated in detail. These include the effects of the finite angular resolution of the instrument, electron-beam space charge, and rotational and thermal motion of the target molecules. From a consideration of the geometry of the ion-detection system and electron beam, the first effect was found to introduce a 0.5% correction term,[17] i.e., the error produced by the finite angular resolution is negligible. Calculations of the last three effects showed that these depend on ion energy and introduce an isotropic term in the angular distribution which is less than 1.0% of the amplitude of the anisotropic component if $E_0 \gg kT$, a condition well satisfied in the present experiment. For example, when the initial thermal velocity of the molecule is added in and an average performed over all directions and magnitudes of this velocity assuming a Maxwellian distribution, a $\cos^2\theta$ distribution distorts to a $\cos^2\theta + 0.01$ distribution when $E_0 = 1.0$ eV and $T = 300\,°\mathrm{K}$, i.e., an isotropic term is introduced which is 1.0% of the amplitude of the $\cos^2\theta$ term. These considerations indicate that instrumental factors are not responsible for the large isotropic term observed here.

Due to the relatively wide energy spread of the electrons and the errors associated with the determination of the electron and ion energy scales, it is possible that a significant portion of the ions ob-

served were actually formed at as much as a volt above threshold. Above threshold, an isotropic term is introduced by averaging the cross section over all magnitudes and orientations of the momentum change vector $\vec{K}$. The magnitude of the isotropic term may increase rapidly with energy above threshold, and this undoubtedly is responsible for at least a small part of the isotropic term which is observed. If large-angle scattering becomes rapidly more probable above threshold, then from Eq. (6) the angular distribution should quickly become more isotropic and eventually distort to a $\sin^2\theta$ character as $\theta' \to 90°$. However, examination of the results of Dunn and Kieffer, [2] as well as comparison with Zare's[4] calculation, indicate that this change is not rapid enough to explain the degree of isotropy observed here. This was verified in the present experiment, where measurements made at electron energies between 29.0 and 38.0 eV, corresponding to the range of thresholds for formation of H^+ ions of different kinetic energies (see Fig. 1, Ref. 2), showed that the angular distribution was rather insensitive to energy, consistent with the energy-distribution data shown in Fig. 6. The degree of anisotropy defined by the ratio $I(23°)/I(90°)$ was slightly greater at low energies than at high energies. For $E_e = 29.0$ eV, $I(23°)/I(90°) = 3.5$ and for $E_e = 38.0$ eV, $I(23°)/I(90°) = 2.9$. This is expected, since at higher electron energies, ions produced above threshold contribute more heavily to the observed ion count because of the fairly wide energy spread in the electron beam. A plausible explanation for the isotropic term is the existence of another process which contributes to H^+ formation with nearly the same appearance potential as that for dissociative ionization from the repulsive $^2\Sigma_u^+$ state. To explain a discrepancy between the observed and calculated kinetic-energy distribution of H^+ from H_2 (see Fig. 2), Kieffer and Dunn[9] have proposed that some of the H^+ is formed by autoionization from repulsive high-lying Rydberg states of H_2.

The observations of Kieffer and Dunn were verified in this experiment, and, in addition, the dependence of the shape of the distribution curves on electron energy was obtained as illustrated by the results in Figs. 3 and 4. The observed energy distribution at $E_e = 150$ eV is definitely wider than that predicted from Franck-Condon overlaps. There are relatively more ions at both high and low energies than theory predicts.[18] Moreover, there is obvious structure on the low-energy side of the curves for both H^+ and D^+ which strongly suggests the existence of another process. An enhancement of the relative numbers of ions with kinetic energy below 7.0 eV becomes more apparent at $E_e = 150$ eV, and at $E_e = 300$ eV a peak at 6.0 eV is a dominant characteristic of the distribution. Measurements of the appearance potentials of ions with both high and low kinetic energy agreed with the results found by Kieffer and Dunn, [9] i.e., there was no observed structure in the ionization efficiency curves above threshold to indicate the onset of a new process. The appearance potential measurements included electron energies up to 60 eV.

As mentioned previously, the degree of anisotropy in the angular distribution of H^+ (D^+) changed only slightly as the threshold energy was varied. This observation suggests that if the isotropic component at threshold is due to another process with about the same appearance potential, then it contributes with nearly equal relative intensity at all energies. The measured angular distribution of D^+ from D_2 at threshold did not differ appreciably from that for H^+. This is expected if the observed dissociation is the result of a direct transition to a repulsive electronic state, since the electronic states of H_2^+ and D_2^+ are identical assuming validity of the Born-Oppenheimer separation. On the other hand, if autoionization contributes heavily to the process, an isotope dependence for the angular distribution would be possible since the autoionization probabilities for H_2 and D_2 may be different. The fact that there was no discernible isotope effect implies that the condition $\Gamma\tau \gg 1$ holds for both H_2 and D_2, where Γ is the autoionization transition probability and τ is the period of nuclear motion proportional to $(\mu)^{1/2}$, where μ is the reduced mass of molecule. This means that the width of the autoionizing state of the molecule is large; hence the probability of a radiationless ionizing transition is also very high, such that nearly all molecules decay from this state via autoionization.

V. CONCLUSION

The results obtained in this experiment have demonstrated the importance of molecular recoil in determining the energy and angular distributions in the laboratory reference frame of protons and deuterons produced by dissociative ionization of H_2 and D_2. A direct measurement made of the recoil momentum of the heavy particles along the beam direction showed that it remains essentially constant from threshold up to 300 eV. No satisfactory theoretical explanation has been found for this observation, although the results do not appear to be physically unreasonable. A complete theoretical description of the effect is complicated by the fact that the final momentum is divided up among four outgoing particles.

When the measured angular distribution of H^+ (D^+) at threshold is corrected to the center-of-mass system, the result is found to contain an isotropic term plus an anisotropic component which does not

fit a $\cos^2\theta$ dependence. If the observed ion count is due to only the $^1\Sigma_g^+ \rightarrow {}^2\Sigma_u^+$ transition, then these results indicate a violation of Dunn's selection rules[1] which predict a vanishing cross section at $\theta = 90°$. Moreover, they demonstrate that the dipole limit does not apply for this process and that the deviation from this approximation follows the form suggested by Zare.[4] Since a large part of the incident electron's momentum is imparted to the heavy particles, even for energies much above threshold, it is doubtful that the momentum change vector $\vec{K}$ is the proper assignment for symmetry axis which defines the angular distribution for dissociative ionization.

The effect of the ejected electron plus a possible rapid change in the most probable direction of the momentum change vector $\vec{K}$ with energy might explain part of the observed isotropic component. Energy-dependence measurements, reported here as well as in an earlier experiment,[2] suggest that this is a small effect. A possible explanation is found in postulating the existence of a process other than excitation to the $^2\Sigma_u^+$ repulsive state of H_2^+ which has nearly the same appearance potential as this process. Kieffer and Dunn[9] have proposed that autoionization from repulsive high-lying Rydberg states of H_2 may contribute significantly to the production of H^+ (D^+) by dissociative ionization. This explanation appears to be consistent with their measurements of the appearance potentials and kinetic-energy distributions of H^+ (D^+) ions from H_2 (D_2) which were verified here. The lack of an observed isotope effect in the angular distribution argues against autoionization, but does not eliminate this possibility.

ACKNOWLEDGMENTS

The authors are indebted to Dr. G. H. Dunn and Dr. R. N. Zare for their valuable suggestions and continued interest ir this work.

---

*Work supported in part by the Advanced Research Projects Agency of the Department of Defense and monitored by Army Research Office, Durham under Contract No. DA-31-124-ARO-D-139.

†Present address: Department of Physics, University of Virginia, Charlottesville, Va.

‡Staff member, Laboratory Astrophysics Division, National Bureau of Standards.

[1]G. H. Dunn, Phys. Rev. Letters 8, 62 (1962).

[2]G. H. Dunn and L. J. Kieffer, Phys. Rev. 132, 2109 (1963).

[3]V. N. Sasaki and T. Nakao, Proc. Imp. Acad. (Tokyo) 11, 413 (1935); 17, 75 (1941).

[4]R. N. Zare, J. Chem. Phys. 47, 204 (1967).

[5]E. H. Kerner, Phys. Rev. 92, 1441 (1953).

[6]H. Ehrhardt, M. Schulz, T. Takaat, and K. Willmann, Phys. Rev. Letters 22, 89 (1969).

[7]H. Ehrhardt, K. H. Hesselbacher, and K. Willmann, in *Proceedings of the Sixth International Conference on the Physics of Electronic and Atomic Collisions* (MIT Cambridge, Mass., 1969), pp. 217–219.

[8]C. E. Kuyatt and J. Arol Simpson, Rev. Sci. Instr. 38, 103 (1967).

[9]L. J. Kieffer and G. H. Dunn, Phys. Rev. 158, 62 (1967).

[10]L. J. Kieffer and R. J. Van Brunt, J. Chem. Phys. 46, 2728 (1967).

[11]Transformation to the center-of-mass system gives the relationship $d\theta \simeq [1 + (m_e E_e/ME_0)^{1/2}\cos\Theta]d\Theta$ between corresponding laboratory and center-of-mass angles Θ and θ provided $(m_e E_e/ME_0)^{1/2} \ll 1$. Since ions observed between angles Θ and $\Theta + d\Theta$ in the laboratory correspond to ions formed between θ and $\theta + d\theta$, the second term in the brackets produces an asymmetry in the laboratory angular distribution which for the energies encountered here gives roughly a 5% effect.

[12]H. S. W. Massey, in *Encyclopedia of Physics*, edited by S. Flügge (Springer-Verlag, Berlin, 1956), Vol. 36, p. 356.

[13]H. S. W. Massey, *Electronic and Ionic Impact Phenomena* (Oxford U. P., London, 1969), Vol. 2, p. 830.

[14]G. Herzberg, *Spectra of Diatomic Molecules* (Van Nostrand, Princeton, N. J., 1950), p. 241.

[15]R. N. Zare and D. R. Herschbach, Proc. IEEE 51, 173 (1963).

[16]If the theoretical value $1.6(1/a_0)$ is used instead of the observed value, the shape of the curve is changed only slightly and the fit to the data is still quite good.

[17]For details of these calculations see R. J. Van Brunt, thesis, University of Colorado, 1969 (unpublished).

[18]Part of the discrepancy between the observed and calculated energy-distribution curves may result from broadening due to the effect of the transverse component of momentum transfer. Small variations in broadening as a function of angle suggested that this is the case; however, because of the relatively poor resolution of our spectrometer and the complexity of the unfolding problem no attempt was made to extract information about the transverse recoil.